

EVALUATION OF TAPM USING THE INDIANAPOLIS (URBAN) AND KWINANA (COASTAL) FIELD DATA SETS

Ashok K. Luhar and Peter J. Hurley

CSIRO Atmospheric Research, PMB 1, Aspendale, Victoria 3195, Australia

Summary

The Air Pollution Model (TAPM) is evaluated using the 1985 Indianapolis (USA) and the 1995 Kwinana (Australia) point-source dispersion data sets, both taken in relatively flat terrain. The first represents urban dispersion, while the Kwinana data set represents coastal dispersion (including fumigation). The model is run with multi-level nesting, both with and without wind data assimilation. Various statistical measures are used to evaluate model performance. Comparison with (published) results obtained from other commonly used models, namely ADMS3, AERMOD and ISCST3, that have been applied to the Indianapolis data set with the observed meteorology, indicates that TAPM performs as well as, if not better than, the best of these models. Comparison with the Kwinana data shows that TAPM performs well in simulating coastal effects, such as sea breezes, fumigation and wind direction shear.

Keywords: TAPM, coastal dispersion, urban dispersion, model evaluation, air pollution modelling, Indianapolis study, Kwinana study, field data.

1. Introduction

CSIRO's The Air Pollution Model (TAPM) is a PC-based, three-dimensional, nestable, prognostic meteorological and air pollution model, driven by a graphical user interface. A complete description of version 2.0 of the model used here is given by Hurley (2002). The model uses global input databases of terrain height, land use, sea-surface temperature, and synoptic meteorological analyses.

TAPM is evaluated using two field data sets on point-source plume dispersion: the 1985 Indianapolis (USA) data set and the 1995 Kwinana (Australia) data set. The former is one of the four data sets that are part of the Model Validation Kit resulting from the European initiative on "Harmonisation within Atmospheric Dispersion Modelling for Regulatory Purposes" (Olesen 1995). The Kit facilitates a standard and uniform comparison of model results. An aim of the present work is to examine the performance of TAPM *vis-à-vis* other commonly used models that have also been tested with the Indianapolis data set. Comparison with the Kwinana data relates to model testing under sea-breeze conditions that are not represented by the Kit.

2. Field Data Sets

2.1. Indianapolis

A full description of the Indianapolis field study, conducted during September–October, 1985, is given in

TRC (1986). It involved sulfur hexafluoride (SF_6) tracer releases from the 83.8 m stack (with diameter 4.72 m) at the Perry K power plant on the south-west edge of Indianapolis, Indiana, USA. The geographic coordinates of this stack are UTM-E 571.40 km ($86^\circ 12'$ W) and UTM-N 4401.59 km ($39^\circ 48'$ N), with the surrounding terrain being relatively flat. The stack is located in a typical industrial/commercial/urban complex with many buildings within one or two kilometres (roughness length of about 1 m).

Meteorological observations were taken at a height of 94 m at the top of a bank building in the middle of the urban area, from two 10-m towers in suburban and rural areas, and from an 11-m tower at an urban location. In addition, vertical meteorological profiles were measured. Hourly-averaged concentrations were observed on a network of up to 160 ground-level monitors on 12 arcs at distances 0.25, 0.5, 0.75, 1.0, 1.5, 2, 3, 4, 6, 8, 10 and 12 km from the stack. To sample the plume, the network of monitors was moved so that it was downwind of the source. Data were taken in 8- or 9-hour test blocks with 19 such blocks altogether. Figure 1 shows the locations of the stack, meteorological sites and the tracer monitors corresponding to the test block 9. A total of 170 hours of tracer data is available, representing all stability classes and most wind speed ranges. Arc-wise maxima were calculated from the crosswind concentration variation, and a quality indicator was assigned to each value. It is recommended that only the data with quality indicator 2 (maxima identified) and 3 (maxima well defined) be used for model comparison. Out of a total of 1511 arc-

hours of data, 1216 are quality 2 and 3, and 469 are quality 3.

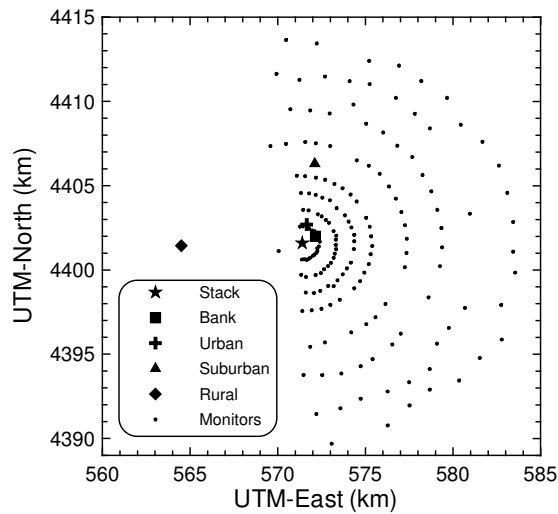


Figure 1. Concentration monitors (Test 9), and meteorological sites for the Indianapolis study.

2.2. Kwinana

Fumigation under south-westerly sea-breeze conditions is a major feature of the summertime air pollution meteorology in the coastal industrial region of Kwinana, south of Perth in Western Australia. Figure 2 presents a map of the Kwinana region in the Australian Map Grid (AMG) coordinate system. An intensive field experiment on fumigation, named the Kwinana Coastal Fumigation Study, was carried out in the region during January–February, 1995 (see Sawford *et al.* 1998). Measurement systems employed during the study included a scanning lidar, an instrumented aircraft, radiosondes, an existing network of air quality stations recording surface-layer meteorology and ground-level sulfur dioxide (SO_2) concentrations, and two sonic anemometers to measure the surface sensible heat flux. Data on emissions from 20 significant point sources of SO_2 in the area, and their physical characteristics, were also obtained. The fumigation aspect of the field study focused mainly on the lidar scanning of buoyant smoke plumes from two stacks, Stage A and Stage C (heights 114 m and 189 m, respectively, and diameters 2.14 m and 2.67, respectively) of the Kwinana Power Station (KPS), which are amongst the dominant SO_2 sources in the area.

The lidar measured vertical cross-sections of individual plumes at several downwind distances, and these scans were then used to derive hourly average dispersion moments both before and after fumigation. The lidar-derived moments contain information about the full three-dimensional structure of the plume.

3. Modelling the Field Data

Since the above two data sets precede the global synoptic meteorological data supplied with TAPM, which are

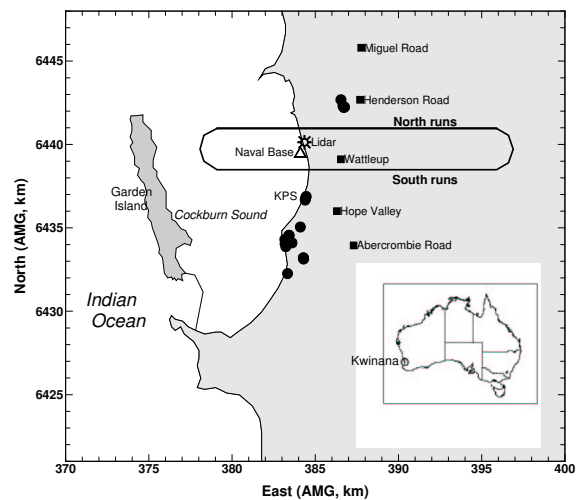


Figure 2. The Kwinana area showing the air quality stations (squares), the lidar, and Kwinana Power Station (KPS) and other SO_2 sources (solid circles).

given from 1997, we used the National Centers for Environmental Prediction (NCEP)/National Center for Atmospheric Research (NCAR) reanalysis data (Kalnay 1996) on horizontal wind components, temperature and moisture, to obtain the required synoptic fields in the model. These data have a horizontal resolution of 2.5° and a temporal resolution of 6 h, while the vertical levels are in a pressure coordinate system with the lowest five levels being 1000, 925, 850, 700 and 600 hPa.

3.1. Application to Indianapolis

TAPM was run for the period 15 September–12 October, 1985, with four nested domains of 30×30 horizontal grid points at 30-km, 10-km, 3-km and 1-km spacing for the meteorology, and 101×101 horizontal grid points at 7.5-km, 2.5-km, 0.75-km and 0.25-km spacing for the pollution, both centred on the stack coordinates. There were 25 vertical levels, with the lowest ten being 10, 25, 50, 100, 150, 200, 250, 300, 400, and 500 m. The Lagrangian mode was used to capture the near-source dispersion more accurately. Two sets of model runs were made: one without data assimilation (i.e. no use was made of observed local meteorology) and the other with data assimilation in which wind speeds and directions observed at the Urban tower (10 m AGL) and the Bank building (94 m) were assimilated into model calculations.

Urban land use dominated the Indianapolis region, and the simulations used the TAPM default urban land-use category (50% hard surface and 50% vegetation/soil with the roughness length of 1 m and an anthropogenic heat flux of 30 W m^{-2}). For Indianapolis data, a value of

0.5 is recommended for the moisture availability factor, which is defined as the ratio of the surface latent heat flux to the total surface heat flux. To match this value, we used a deep soil moisture content of 0.3 kg kg^{-1} .

The hourly average model meteorological predictions on the 1-km spaced grid were extracted at the nearest grid point to each of the monitoring sites and compared with the data. The hourly average pollution predictions on the 0.25-km spaced grid were processed to obtain ground-level concentration maxima at the 12 arcs.

3.2. Application to Kwinana

To simulate the ground-level SO_2 data, TAPM was run for the period 24 January–6 February, 1985, with four nested domains of 30×30 horizontal grid points at 30-km, 10-km, 3-km and 1-km spacing for the meteorology, and 81×81 horizontal grid points at 7.5-km, 2.5-km, 0.75-km and 0.25-km spacing for the pollution, both centred on coordinates AMG-E 384.5 km ($115^\circ 46.5'$ E, longitude) and AMG-N 6437.6 km ($32^\circ 11.5'$ S, latitude). The vertical levels were the same as in the Indianapolis case and the Lagrangian mode was used in dispersion calculations. Model runs were made without and with data assimilation (using wind speeds and directions observed at 10 m and 27 m AGL at the Hope Valley monitoring station). A very dry (summertime) deep soil moisture content of 0.05 kg kg^{-1} was used based on past experience in the Kwinana area.

The default TAPM database values of sea-surface temperature are long-term monthly means. The aircraft measurements taken during the Kwinana study suggest that these values were about 3°C too low, and so they were increased by this amount. The default deep soil temperature values were also increased by this amount.

The hourly average model meteorological and pollution predictions on the smallest respective grids were extracted at the nearest grid point to each of the monitoring sites and compared with the data. Any observed SO_2 concentrations $\leq 2.7 \mu\text{g m}^{-3}$ (detection limit) were not considered in model evaluation statistics.

To simulate the lidar dispersion moments of plumes from Stage A and Stage C, TAPM was run in the two-tracer mode corresponding to the two stack sources for the period 29 January–2 February, 1995. (Fully processed lidar data are available for 30, 31 January, and 2 February.) Data assimilation was employed and a finer resolution of 161×121 horizontal grid points at 3.0-km, 1.0-km, 0.3-km and 0.1-km spacing for pollution calculations was used, keeping the meteorological grids and the vertical levels the same as above. The three-dimensional concentration field $c(x,y,z)$ predicted by TAPM for each stack plume was processed to obtain dispersion moments. The model grid coordinates x and y were converted into locations x' and y' in the wind coordinate system, where x' is the downwind distance aligned along the onshore flow direction at the boundary-layer top and y' is the distance perpendicular to it. The hourly-average dispersion moments about the

mean were calculated, in the vertical direction for example, as

$$\overline{(z - \bar{z})^n (x')} = \frac{\iint (z - \bar{z})^n c(x', y', z) dy' dz}{\iint c(x', y', z) dy' dz}$$

where z is the vertical level height. The direction of the onshore flow, required in the calculation of x' and y' was determined from the model output for a grid located over the sea close to the power station.

4. Model Results

4.1. Indianapolis

Figure 3 compares the time series of the hourly-average wind speed and wind direction observed at 94 m AGL with that predicted by TAPM at the 100-m level with and without wind data assimilation. It is evident that even without data assimilation, the model performs well in simulating the observed variation. This also shows that the NCEP synoptic data used in the model are robust and reliable. The model also performs well at the other sites and for other meteorological and turbulence parameters governing dispersion (plots not shown).

The quantile-quantile (Q-Q) plot in Figure 4 compares the model concentration distribution with the observed one (Quality 2 & 3). In this plot, the sorted observed values are plotted against the sorted model values (i.e. independent of time and position), which graphically depicts any model bias over the frequency distribution. The model shows bias towards distribution underprediction for the lowest concentrations, which then shifts to overprediction from about $300 \text{ ng m}^{-3} (\text{g s}^{-1})^{-1}$. The two curves separate at about $450 \text{ ng m}^{-3} (\text{g s}^{-1})^{-1}$, and the subsequent variation indicates that at the extreme end the model overpredicts by about 25% without assimilation and by about 10% with assimilation.

Table 1 gives model performance statistics recommended by the Model Validation Kit, for TAPM. Also given are these statistics, reported in McHugh *et al.* (1999), for the regulatory models ISCST3 (USA), AERMOD (USA) and ADMS3 (UK). It is clear that the mean is best predicted by TAPM (without data assimilation) followed by ADMS3 and TAPM-A (with data assimilation), but the differences between these values are not significant. The correlation coefficient is the highest for TAPM-A followed by TAPM and ADMS3, while the factor-of-two (fraction of predictions within a factor of two of observations) measure shows that ISCST3 performs the best, but other measures show that this model performs poorly. The factor-of-two values are a little lower for TAPM than for any other model. This is mostly because in TAPM occasionally the plume does not mix down to the ground under nighttime stable conditions, while the observations show otherwise. In all other models, *observed* meteorological, stability and turbulence data are used as inputs with the

assumption that the minimum value of the Monin-Obukhov length is 50 m during stable conditions, which moderates the stability (to account for urban effects) and causes the plume to diffuse more and reach the ground. Overall, AERMOD performs better than ISCST3 but the three top performing models are TAPM-A, TAPM and ADMS3. The fact that TAPM performs well without data assimilation is very encouraging because it indicates that the model can be used successfully without any direct meteorological observations from the site.

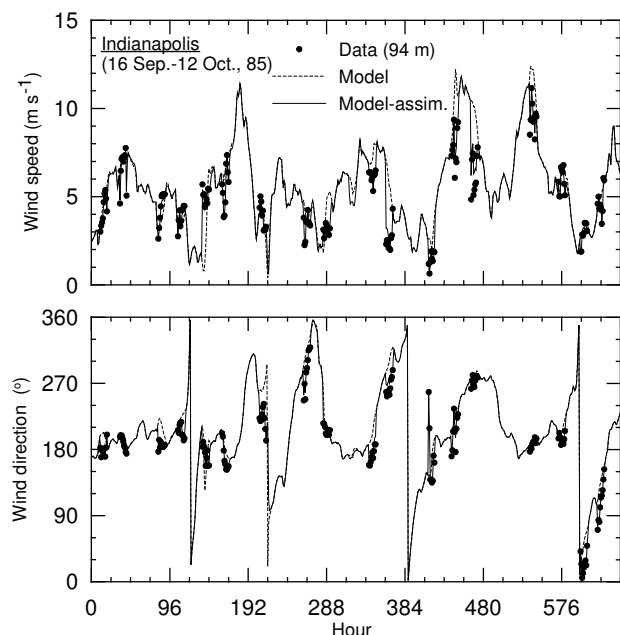


Figure 3. Time series of the hourly-average wind speed and wind direction observed at 94 m AGL and that predicted by TAPM at the 100-m level with and without wind data assimilation.

4.2. Kwinana

The time series of the hourly-average wind speed and wind direction observed at 10 m AGL at the Hope Valley station and the predictions by TAPM at the same level with and without wind data assimilation are shown in Figure 5. TAPM simulates both wind speed and wind direction data very well, including the change in wind direction to the west/south-west during the day on most days, which corresponds to the onset of sea breeze that turns more southerly (i.e. anticlockwise) with time. There are some differences between wind speeds obtained with and without data assimilation, especially close to the start and end times of the simulated period. The model also performs well at the other sites and for other meteorological parameters (plots not shown).

The Q-Q plot shown in Figure 6 indicates that there is a bias in the model to underpredict concentration distribution at very low values (below about $10 \mu\text{g m}^{-3}$) and to overpredict all higher concentration levels. The data assimilation and no-assimilation curves are similar except for the highest three concentrations where the

overprediction by the no-assimilation case is larger. Most of the high concentration events at the five sites occur under sea-breeze conditions. Small differences in meteorological conditions, especially in wind direction, can lead to large differences in high-end concentrations at fixed sites downwind of point sources. This also means that the top few model concentrations with and without data assimilation do not necessarily correspond to the same events.

The performance statistics given in Table 2 shows a reasonable performance by TAPM in predicting concentrations at the five monitoring stations in

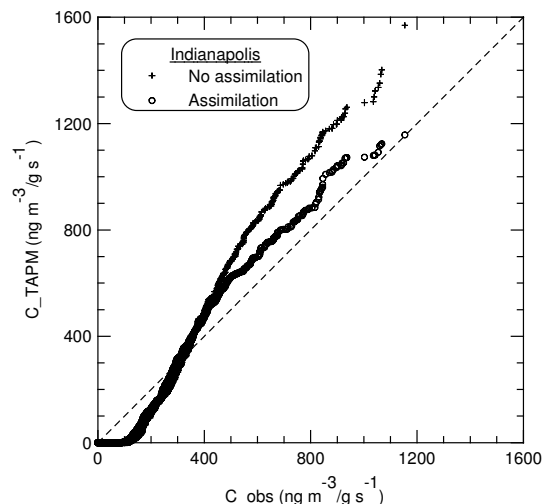


Figure 4. Q-Q plot of the predicted vs. observed concentrations with and without data assimilation.

Kwinana, especially as they are paired in both space and time. The Sigma values suggest that the model values are more scattered than the observed data. Data assimilation leads to an improvement in the prediction accuracy, but the no-assimilation results look satisfactory too.

Figure 7 compares of the downwind variation of the lidar-derived plume spreads [$\sigma_z = ((z - \bar{z})^2)^{1/2}$ and $\sigma_y = ((y - \bar{y})^2)^{1/2}$] with the model predictions for the neutral case of fumigation (in which the dispersion above the thermal internal boundary layer (TIBL) takes place in a neutrally stratified layer). More details of the data and fumigation cases are given in Luhar and Young (2002). (The stable fumigation cases were not compared here since the diffusion of the plume in the stable layer prior to its fumigation was too small to be resolved by the chosen grid resolution in the model.)

There are seven hours of data corresponding to the model hours: 1500, 1600 h on 30 January; 1400, 1500, 1600 h on 31 January; and 1400, 1500 h on 2 February, with the last one involving the tall stack (Stage C) while the rest involve the small stack (Stage A). The normalised downwind distance in Figure 7 is $X = (x'/u_o)(w*/z_e)$ and the moments are scaled by z_e . The

same values of z_e (TIBL height in the fumigation zone), w_* (convective velocity) and u_o (mean wind speed within the TIBL) used by Luhar and Young (2002) were used here for scaling. In Figure 7a, the model and lidar vertical spreads display similar behaviours, both showing an initial increase ($X \leq 1.3$) due to plume buoyancy and then to the plume material spreading out within the TIBL

Table 1. Model performance statistics for Indianapolis, Quality 2&3 ($N_{\text{obs}} = 1216$)

Model	Mean $\text{ng m}^{-3} (\text{g s}^{-1})^{-1}$	Sigma $\text{ng m}^{-3} (\text{g s}^{-1})^{-1}$	Bias $\text{ng m}^{-3} (\text{g s}^{-1})^{-1}$	NMSE	Cor	Fa2	Fb	Fs
C_OBS	258	222	0.0	0.0	1.00	1.00	0.00	0.00
TAPM	261	335	-2.8	1.4	0.46	0.32	-0.01	-0.41
TAPM-A	248	284	9.6	1.0	0.51	0.36	0.04	-0.25
ISCST3	404	321	-146.4	1.4	0.16	0.45	-0.44	-0.37
AERMOD	225	196	33.2	1.3	0.17	0.41	0.14	0.13
ADMS3	265	255	-7.5	1.3	0.26	0.42	-0.03	-0.14

NMSE = normalised mean square error, Cor = correlation coefficient, Fa2 = factor of two, Fb = normalised bias, Fs = normalised sigma

Table 2. Model performance statistics for Kwinana ($N_{\text{obs}} = 498$)

Model	Mean $\mu\text{g m}^{-3}$	Sigma $\mu\text{g m}^{-3}$	Bias $\mu\text{g m}^{-3}$	NMSE	Cor	Fa2	Fb	Fs
C_OBS	15.3	19.1	0.0	0.0	1.00	1.00	0.00	0.00
TAPM	14.7	28.8	0.6	3.3	0.42	0.20	0.04	-0.41
TAPM-A	15.8	27.9	-0.5	2.4	0.54	0.26	0.03	-0.38

under fumigation. σ_y/z_e eventually reaches a near-constant value as the bulk of the plume material becomes trapped within the slow-growing TIBL. At larger distances, the model spreads are larger than the data, probably due to the fact that the undulating terrain between the lidar and the plume prevented the sampling of the lower edges of the plume at such distances.

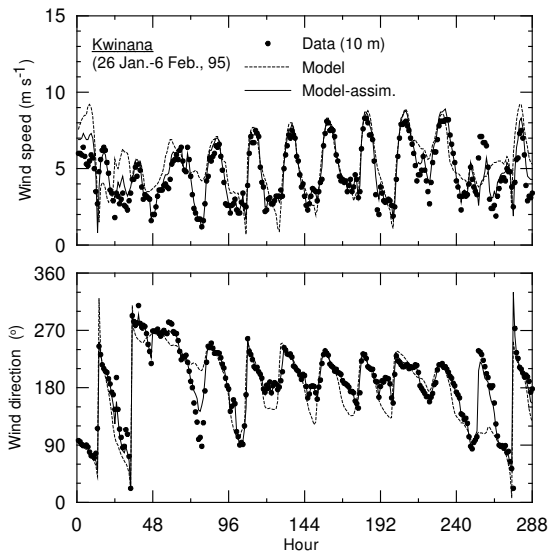


Figure 5. Time series of the hourly-average wind speed and wind direction observed at 10 m AGL at the Hope Valley station and that predicted by TAPM at the same level with and without wind data assimilation.

In Figure 7b, most model lateral spreads, σ_y/z_e , agree with the lidar data. The initial abnormal behaviour in the

three model curves, showing a decreasing or near constant σ_y/z_e , is due to the coarse horizontal resolution ($100 \text{ m} \times 100 \text{ m}$) used in the model, which is unable to resolve the plume. (These parts of the curves were not considered in calculating the lateral skewness shown below.) The large variation between the model curves is largely due to the large variation in the magnitude of shear between these cases, and also to the fact that the distance at which the plume is entrained into the TIBL is different.

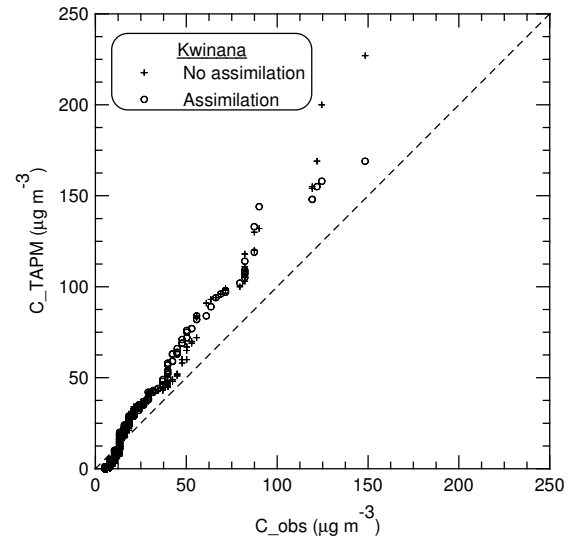


Figure 6. Q-Q plot of the predicted vs. observed concentrations with and without data assimilation.

Figure 8a presents the lidar data and model curves of the mean vertical skewness $Sk_z [= ((z - \bar{z})^3) / \sigma_z^3]$. The

main feature of the observed skewness is that it reaches a peak magnitude of -1 at about $X = 1$ (the distance at which the plume is fumigating) and then gradually approaches zero in the far field. Here, a negative Sk_z implies that the concentration distribution has a peak close to the top of the boundary layer with a tail towards the ground which is consistent with the classic fumigation concentration distribution. The skewness approaches zero as the bulk of the plume material is entrained into the TIBL and becomes well mixed. The model describes the lidar data well for the overall range of distances.

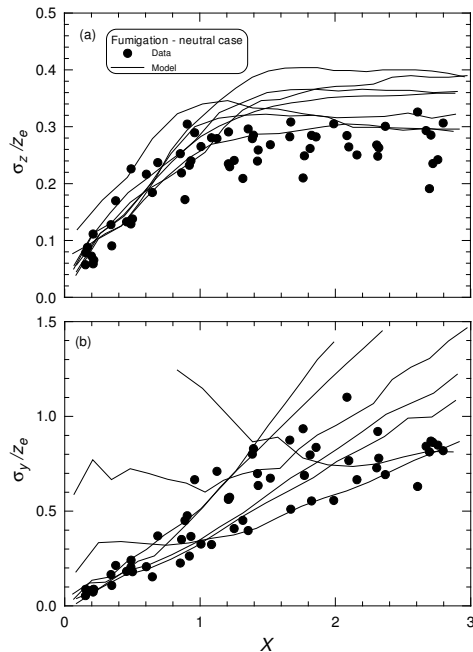


Figure 7. The lidar and model variations of the normalised vertical and lateral spreads. The model curves correspond to different hourly periods.

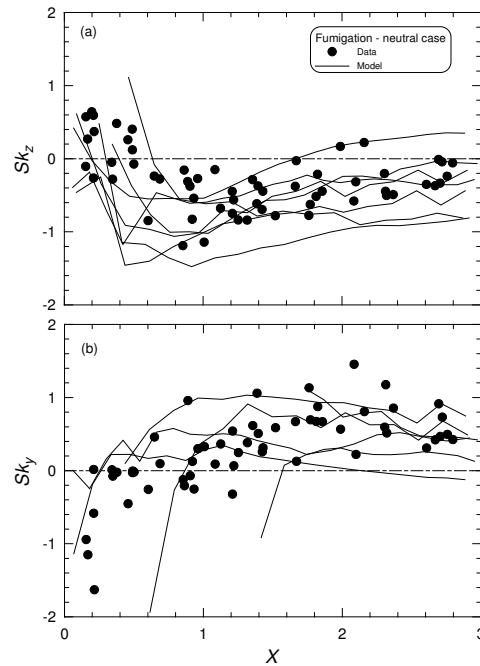


Figure 8. The lidar and model variations of the vertical and lateral skewnesses. The model curves correspond to different hourly periods.

The lidar skewness in the lateral direction, Sk_y , presented in Figure 8b is clearly positive beyond about $X = 1$, with a mean value of 0.7. The observed positive skewness in the fumigation zone is due to the vertical wind direction shear within the TIBL, which is well reproduced by the model.

5. Conclusions

The Air Pollution Model (TAPM) was evaluated using the Indianapolis (urban) and the Kwinana (coastal) field data sets on point source plume dispersion in relatively flat terrain. As expected, TAPM performed better when the data assimilation option was used, but the results without data assimilation were also good. The latter is encouraging because in this case the model does not require any direct meteorological observations (which are often not available). Comparison with (published) results obtained using ADMS3, AERMOD and ISCST3 for Indianapolis (with observed meteorology) indicates that TAPM performs as well as, if not better, than the best of these models. Comparison with the Kwinana SO_2 and lidar data set shows that TAPM also can simulate coastal effects, such as sea-breeze onsets and fumigation cases with vertical wind direction shear, well.

Acknowledgments

The authors thank Mark Collier and Mary Edwards for generating the NCEP/NCAR analyses in TAPM format.

References

- Hurley P. 2002, *The Air Pollution Model (TAPM) Version 2. Part 1: Technical Description*. CSIRO Atmospheric Research Technical Paper.
- Kalnay E. et al. 1996, 'The NCEP/NCAR 40-Year Reanalysis Project', *Bull. Amer. Meteorol.* **77**:437–71.
- Luhar A. K. and Young S. A. 2002, 'Dispersion moments of fumigating plumes—lidar estimates and PDF model simulations', *Bound.-Layer Met.*, in press.
- McHugh C. A., Carruthers D. J., Higson, H. & Dyster S. J. 1999, 'Comparison of model evaluation methodologies with application to ADMS3 and US models', *6th International Conf. on Harmonisation within Atmospheric Dispersion Modelling for Regulatory Purposes*, Rouen, France, 11–14 October.
- Olesen H. R. 1995, 'The Model validation exercise at Mol: overview of results', *Int. J. Environ. Pollut.* **5**:761–84.
- Sawford B. L., Luhar A. K., Hacker J. M., Young S. A., Yoon I.-H., Noonan J. A., Carras J. N., Williams D. J. & Rayner, K. N. 1998, 'The Kwinana coastal fumigation study: I. Program overview, experimental design and selected results', *Bound.-Layer Met.* **89**:359–84.
- TRC 1986, *Urban Power Plant Plume Studies*, EPRI Report EA-5468, EPRI, 3412 Hillview Ave, Palo Alto, CA 94304.